RSC Advances

ROYAL SOCIETY OF CHEMISTRY

PAPER

View Article Online
View Journal | View Issue

Check for updates

Cite this: *RSC Adv.*, 2025, **15**, 7855

Role of metal(II) hexacyanocobaltate(III) surface chemistry for prebiotic peptides synthesis†

Babita Saroha,[a] Anand Kumar, *[b] Indra Bahadur, *[c] Devendra Singh Negi,[d] Monika Vats,[e] Ashish Kumar,[f] Faruq Mohammad [g] and Ahmed Abdullah Soleiman[h]

Double metal cyanide (DMC), a heterogeneous catalyst, provides a surface for the polymerization of amino acids. Based on the hypothesis, the present study is designed to evaluate favorable environmental conditions for the chemical evolution and origin of life, such as the effects of temperature and time on the oligomerization of glycine and alanine on metal(II) hexacyanocobaltate(III), MHCCo. A series of MHCCo complexes were synthesized and characterized by XRD and FT-IR techniques. The effect of outer metal ions present in the MHCCo complexes on the condensation of glycine and alanine was studied. Our results revealed that Zn^{2+} ions in the outer sphere showed high catalytic activity compared to other metal ions in the outer sphere. Manganese(II) hexacyanocobaltate(III) (MnHCCo), iron(II) hexacyanocobaltate(III) (FeHCCo), nickel(II) hexacyanocobaltate(III) (NiHCCo) complexes condense the glycine up to trimer and the alanine up to dimer. At the same time, ZnHCCo showed the most valuable catalytic properties that change glycine into a tetramer and alanine into a dimer with a high yield at 90 °C after four weeks. ZnHCCo showed high catalytic activity because of its high surface area compared to other MHCCo complexes. High-Performance Liquid Chromatography (HPLC) and Electron Spray Ionization-Mass Spectroscopy (ESI-MS) techniques were used to confirm the oligomer products of glycine and alanine formed on MHCCo complexes. The results also exposed the catalytic role of MHCCo for the oligomerization of biomolecules, thus supporting chemical evolution.

Received 9th January 2025
Accepted 17th February 2025

DOI: 10.1039/d5ra00205b

rsc.li/rsc-advances

Open Access Article. Published on 12 March 2025. Downloaded on 2/9/2026 5:05:38 PM.
This article is licensed under a Creative Commons Attribution-NonCommercial 3.0 Unported Licence.

1. Introduction

Amino acids are relevant to the formation of biopolymers which eventually lead to life.[1–4] The monomers of proteins, amino acids, are found both in terrestrial life as well as in meteorites.[5–9] In addition, it was further explored by Ikehara and coworkers in the [GADV]–protein world hypothesis that primitive peptides were composed of four amino acids GADV—glycine/alanine/aspartic acid/valine.[10] On primitive Earth the first molecular oligopeptide informational replicator has consisted of Glu-Gly-Gly-Ser-Val-Val-Ala-Ala-Asp;[11] similarly, Gulik also reported Asp-Ala-Lys-Val-Gly-Asp-Gly-Asp chain as the first oligopeptide informational replicator.[12] GADV concentrations of more than 10^{-2} M were found in Miller's "soup" as well as in extraterrestrial meteorites.[13–16] By activating an electric discharge in a highly reducing gas mixture of CH_4, NH_3, and H_2, which at the time was believed to be representative of the primitive atmosphere, Miller synthesized some amino acids, including Gly, Ala, and Asp along with two non-proteinones, β-alanine and amino-*n*-butyric acid.[17,18] According to the Haden Eon hypothesis for the prebiotic organic compound synthesis and the emergence of life, volcanic island lighting is crucial. The amount of exposed sub-aerial land was around 12%.[19] A volcanic island eruption released plumes of hot pebbles and soot, as well as water vapors and other gases (*e.g.*, H_2, NH_3, CO, CO_2, CH_4, SO_2, H_2S) at regular intervals, creating a reducing atmosphere;[20] concurrently, electric discharge in the form of high-intensity lightning was also rife within the plumes. The exceptionally high temperature, together with the electrified lightning within the plume, helped to break bonds of gases generating unstable and highly charged free radicals (formyl, HCO; and hydroxymethyl, CH_3O and CH_2O; and hydroxyl, OH) as well as ions (*e.g.*, hydroxyl ions, OH^-; ammonium ion, NH_4^+). Highly unstable chemical radicals, upon recombining, within the plume synthesized HCN, aldehydes, ketones, formic acid,

[a]*School of Biological sciences, Doon University, Dehradun, 248001 (UK.), India*
[b]*Department of Chemistry, SGRR (PG) College, Dehradun, 248001 (UK.), India. E-mail: anandkciitd17@gmail.com*
[c]*Department of Chemistry, North-West University (Mafikeng Campus), Private Bag X2046, Mmabatho 2735, South Africa. E-mail: bahadur.indra@nwu.ac.za*
[d]*Department of Chemistry, H. N. B. Garhwal University, Srinagar, 246174 (UK.), India*
[e]*Department of Chemistry, Dhanauri (PG) College, Dhanauri, Haridwar, 247667 (UK.), India*
[f]*Department of Chemistry, H. N. B. Government (PG) College, Udham Singh Nagar, Khatima, 262308 (UK.), India*
[g]*Department of Chemistry, College of Science, King Saud University, P.O. Box 2455, Riyadh11451, Kingdom of Saudi Arabia*
[h]*Department of Chemistry, Southern University and A&M College, Baton Rouge, LA 70813, USA*

† Electronic supplementary information (ESI) available. See DOI: https://doi.org/10.1039/d5ra00205b

© 2025 The Author(s). Published by the Royal Society of Chemistry

Open Access Article. Published on 12 March 2025. Downloaded on 2/9/2026 5:05:38 PM. This article is licensed under a Creative Commons Attribution-NonCommercial 3.0 Unported Licence.

etc.[21] The prebiotic soup would likely have been extremely diluting concerning amino acid concentrations varying from 4×10^{-3} M to 10^{-7} M.[22,23] Amino acids and their condensation products (dipeptides, tripeptides, all the way to oligopeptides) are one of the key events during prebiotic chemistry.[24] Thus, the study of the key reactions is very important.[25–28]

Oligomerization of amino acids was the next necessary step in the emergence of life. The major challenges have to do with the low concentration and the short half-life of amino acids. So, how could this feat of oligomerization be accomplished? One way is to understand the role played by minerals/metal oxides/double metal cyanide (DMC) complex.[27,29–31] In addition, to work out the effect of temperature, pH, concentration, salinity, *etc.*, the adsorption of amino acids on the surface of minerals/metal oxides/DMC.[27,28,32–45]

Clays (*e.g.*, kaolinite and montmorillonite) are composed of various minerals, which are widely accepted to act as heterogeneous catalysts for the condensation of amino acids—*i.e.*, peptide bond formation. It is believed that such clay-minerals were present on very early Earth approximately 4.3 billion years ago.[46–51] The principal thing about clay minerals is that they are charged both on the external and internal surfaces and thus could have acted as templates for specific adsorption of their surfaces, allowing the condensation to proceed[52–56] *i.e.*, allowing oligomerization to take place. Egami (1975) and Hazen (2021) reported that the concentration of minor transition elements (Mo, Zn, Fe, Cu, Mn, and Co) in the primordial sea to be 7–100 nM.[57,58] In addition, Fe^{2+}, Mg^{2+}, Mn^{2+}, Co^{2+}, Ni^{2+}, Cu^{2+}, and Zn^{2+} are all metal ions very frequently present in enzymes of extant biology.[59] Metal ions reduce the barrier of reaction involved as compared to the case where no metal ions are involved. Coordination of metal ions with the electronegative atoms in the reactants polarizes the C=O bond and thus enhances the attack of nitrogen carrying molecules, thus results in effortless formation of the simplest peptide linkages in the interstellar medium. Bond energy of metal oxygen and the charge on the metal ions are the vital factors.[60a,b] Similarly metal ions have played a role for glycine and alanine polymerization.[61] Cyanide has been reported as a product in several simulated prebiotic experiments and is supposed to have been readily available under primitive Earth conditions.[62,63] Miller estimated the HCN concentration in the prebiotic oceans to be higher than ~4.00 μM; this concentration depended on the rate of HCN formation at the early hydrothermal vents; its stability in the early ocean-water; and then its eventual degradation due to the sun's rays impinging on the surface water. HCN is an important organic molecule for synthesizing many prebiotic molecules, including amino acids and nucleobases.[64] This is because the cyanide ions (CN^-) stabilized due to the formation of insoluble DMC complexes.[65,66] The clay surface absorbed DMC complexes help to concentrate monomers (in this case amino acids), allowing oligomerization to proceed by acting as a catalyst.[67–70] Similarly, a series of metal(II) hexacyanocobaltate(III) (MHCCo) complexes formed in the primordial sea settle on the seashores, where they make their surfaces available for further interaction, such as oxidation.[67,71]

In this paper, we evaluated the catalytic ability of MHCCo complexes for the formation of prebiotic peptides. A series of MHCCo complexe syntheses are described in the current work. The entire experiment is carried out at different temperatures (60 °C to 120 °C) for five weeks. To the best of our knowledge, the role of outer metal ions in MHCCo complexes as catalyst for the oligomerization of amino acids has not been studied in the literature pertaining to the emergence of life on Earth.

2. Materials and method

2.1. Chemicals

Potassium hexacyanocobaltate(III) (Fluka), $Mn(NO_3)_2$ (E. Merck), $Fe(NO_3)_2$ (E. Merck), $Ni(NO_3)_2$ (E. Merck), $Zn(NO_3)_2$ (E. Merck). Sodium hexane sulphonate, H_3PO_4, CH_3CN (HPLC grade), and standard peptides were purchased from Sigma-Aldrich. During the experimental studies, Millipore water was used.

2.2. Preparation of metal hexacyanocobaltate(III)

Kaye and Long, 2005 method,[72] was followed for the synthesis of MHCCo complexes from potassium hexacyanocobaltate(III). 10 mmol of potassium hexacyanocobaltate(III) dissolved in 100 mL Millipore water, was added to the solution of 18 mmol metal nitrate in100 mL Millipore water dropwise. The precipitate formed was allowed to anneal in the mother liquor and filtered through a bucker funnel. The formed precipitate was washed with Millipore water, dried at 60 °C, powdered, and sieved with a 100 mesh size.

2.3. CHN, TGA/DTA, XRD

The Elementar Vario ELHI CHNS analyzer was used for carbon, hydrogen, and nitrogen percentages present in MHCCo complexes. The water crystallization found in MHCCo complexes was monitored by a thermal analyzer. A 10 °C min heating rate was carried out throughout the measurement, while Al_2O_3 as a reference was used. The X-ray diffraction technique was used for the authentication of MHCCo complexes. The relative-intensity data and interplanar spacing (d) were in good agreement with the reported values.

2.4. Infrared spectra

The vibration frequencies of synthesized MnHCCo, FeHCCo, NiHCCo, and ZnHCCo complexes matched the previously reported data.[73–75] The FT-IR spectra of MHCCo complexes were recorded on the KBr pallet on a Perkin Elmer FTIR spectrophotometer.

2.5. Surface area measurement

The surface area of MHCCo complexes was analyzed by the Brunauer–Emmett–Teller (BET) method on a surface area analyzer.[76]

2.6. Reaction method

Initially, 0.1 gram of MHCCo complexes and 0.1 mL of glycine and alanine amino acid (0.01 M) were impregnated separately, and the suspension was dried at 90 °C for 3 h. After drying, it

 © 2025 The Author(s). Published by the Royal Society of Chemistry

Open Access Article. Published on 12 March 2025. Downloaded on 2/9/2026 5:05:38 PM. This article is licensed under a Creative Commons Attribution-NonCommercial 3.0 Unported Licence.

was kept at three different temperatures (60 °C, 90 °C, and 120 °C) separately for the analysis of peptide bond formation and monitored for five weeks, *i.e.* 7, 14, 21, 28, and 35 days. The sample was analyzed weekly. No fluctuating drying/wetting conditions were simulated. Glycine and alanine were used separately for the control experiment by heating at the required temperature in an empty test tube of glass measuring 150 × 15 mm. After the first week, adsorbed amino acids and related reaction products were released by treating peptide condensation products obtained with 1 mL of a 0.1 M calcium chloride solution. The reaction product obtained was centrifuged, and the supernatant was analyzed by HPLC and ESI-MS analysis.

2.7. HPLC analysis

HPLC with a column (Spherisorp 5 μm ODS2 4.6 mm × 250 mm) was used for the product analysis. The product was analyzed at 200 nm wavelength by a UV detector. Sodium hexane sulphonate (10 mM) acidified with H_3PO_4 at a pH of ~2.5 (solvent A) and CH_3CN(solvent B) was used as mobile phase compositions at a 1 mL min^{-1} flow rate. Identification of the obtained products was done by retention times, and later on, co-injection method was used for further elucidation. The yield of the peptide bond formation was calculated by the peak area of the products and a standard comparison (Fig. S1–S4†).

2.8. Electrospray ionization-mass spectrometry analysis

ESI-MS spectral data were recorded on a Bruker MicroTOF-Q II mass spectrometer on positive mode using the direct injection method in the range *m*/*z* 50–500. The mass analysis of the product obtained was recorded by mass spectroscopy equipped with an electrospray ionization (ESI) source. Product ionization was done by following the ESI setting: 10 psi nebulizer gas flow, 300 °C temperature, 4000 V capillary voltage, and 5 L min^{-1} dry gas. In the presence of the ZnHCCo complex, glycine and alanine were heated for four weeks at 90 °C, and the ESI MS spectra of the product were analyzed.

2.9. Field emission scanning electron microscopy FE-SEM

The 2-D imaging, internal structure, and morphology of the complexes MnHCCo, FeHCCo, NiHCCo, and ZnHCCo were analyzed with the help of FE-SEM.

2.10. Statistical analysis

All the experiments were performed in triplicate and the results were recorded as the mean of the triplicate measurements.

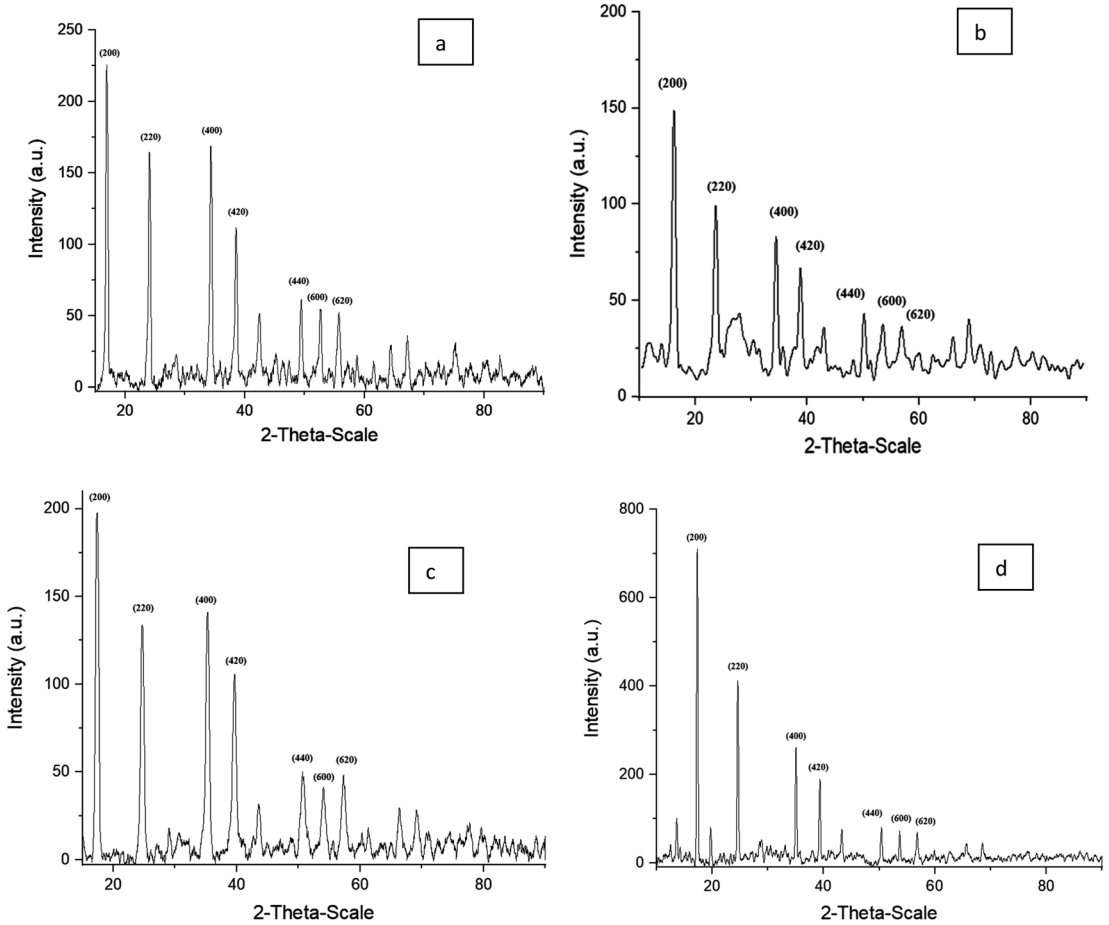

Fig. 1 XRD data of (a) MnHCCo, (b) FeHCCo, (c) NiHCCo, (d) ZnHCCo.

Open Access Article. Published on 12 March 2025. Downloaded on 2/9/2026 5:05:38 PM. This article is licensed under a Creative Commons Attribution-NonCommercial 3.0 Unported Licence.

3. Results and discussion

The first step of material characterization is to identify the purity of the complexes. Fig. 1(a–d) represents MnHCCo, FeHCCo, NiHCCo, and ZnHCCo complex XRD patterns. JCPDS diffraction files are used for analyzing the XRD pattern of MHCCo complexes. The diffraction peaks obtained are carefully matched with the relative intensities of the MHCCo complexes, JCPDS file no. for MnHCCo (22-1167), JCPDS file no. for FeHCCo (89-3736), JCPDS file no. for NiHCCo (22-1184), and JCPDS file no. for ZnHCCo (32-1468). The FT-IR spectrum (depicted in ESI Fig. S5†) of MHCCo complexes showed four significant peaks. In the case of ZnHCCo, the band occurs at 2181 cm^{-1} corresponds to a strong CN stretching frequency; at 1607 cm^{-1} peak represents the O–H bending of interstitial water molecules; 700 cm^{-1} occurs due to the bending of metal-carbon; and at 451 cm^{-1}, it represents the metal-cyanide bending. The broad band appears and ranges from 3382 cm^{-1} to 3430 cm^{-1} which corresponds to coordinated water in MHCCo complexes. The bands that occur due to other MHCCo complexes are indicated in Table 1.

The MHCCo complexes were further characterized by TG/DT analysis. Fig. S6(a–d)† represents the obtained thermograms. With the help of the TG curve of MHCCo complexes, the degree of hydration was calculated. Fig. S6(a)† represents the thermogram for MnHCCo complexes that indicated mass loss which corresponds to nearly two water molecules, the FeHCCo complex showed a mass loss of three water molecules (Fig. S6(b)†), NiHCCo complex showed a mass loss, of three water molecules (Fig. S6(c)†), ZnHCCo complex showed a mass loss of four water molecules (Fig. S6(d)†). The percentages of C, H, and N in the MHCCo complexes were analyzed by CHNS analysis and are depicted in Table S1.† The experimental results obtained by elemental analysis matched the theoretical value. The synthesized MHCCo complexes were analyzed by XRD, CHN analysis, and TG/DTA, as follows:

(1) $Mn_3[Co(CN)_6]_2 \cdot 2H_2O$ (brown);

(2) $Fe_3[Co(CN)_6]_2 \cdot 3H_2O$ (blue);

(3) $Ni_3[Co(CN)_6]_2 \cdot 3H_2O$ (sky blue);

(4) $Zn_3[Co(CN)_6]_2 \cdot 4H_2O$ (white)

Fig. 2(a)–(d) present the FE-SEM images and EDX spectra of MnHCCo, FeHCCo, NiHCCo, and ZnHCCo, respectively.

The structural morphology of FeHCCo, NiHCCo, and ZnHCCo particles appeared spherical and uniform; whereas that of MnHCCo particles appeared to be polygon in shape (the square shape was mostly observed). The particle size of FeHCCo, NiHCCo, and ZnHCCo was found to be uniform, suggesting a narrow size distribution, and that of the MnHCCo particle was found to be non-uniform, suggesting a wide size distribution. Similar morphological characteristics for these complexes have been reported in the literature.[77] The energy dispersive X-ray (EDX) spectra indicate the presence of the corresponding metal in the MHCCo complexes. FeHCCo complexes with spherical morphology are also suggested by Zhang *et al.* (2019).[78]

Table 1 Infrared spectral frequencies (cm^{-1}) of MHCCocomplexes

MHCCo	ν_{CN}	δ_{OH}	δ_{M-C}	δ_{M-CN}
MnHCCo	2170	1610	707	445
FeHCCo	2169	1607	695	456
NiHCCo	2175	1610	699	461
ZnHCCo	2181	1607	700	451

To find the catalyzing properties of the MHCCo complexes, the oligomerization reaction of glycine and alanine was carried out at various temperatures (60, 90, and 120 °C) over a period of five weeks (7, 14, 21, 28, and 35 days) in the presence of MHCCo complexes. We analyzed the effects of temperature and reaction time on the oligomerization of glycine and alanine. The catalytic efficiency of tested MHCCo complexes varied significantly with time and temperature, as shown in Fig. 3(a–c)–6(a–c).

The yields of MHCCo-catalyzed glycine and alanine oligomerization at 60, 90, and 120 °C after five weeks are summarized in Tables 2 and 3. The relationship between product yield and time as a function of temperature follows sigmoidal trend, with yield increasing over time as temperature rises. The yields obtained in the presence of MHCCo complexes were significantly higher than those from the blank experiment. After five weeks, diketopiperazine (DKP) of glycine [DKP (Gly)] and a dimer of glycine, Glycyl-glycine $(gly)_2$ was detected in glycine experiments without catalyst, whereas no peptide formation was obtained in alanine experiments without catalyst. The formation of DKP(Gly), and $(gly)_2$ along with the absence of alanine condensation in control experiments, aligns with previous studies.[79,80] this suggested that MHCCo complexes provide a catalytic surface for the thermal condensation of glycine and alanine, facilitating oligomerization within a relatively short time at temperature below 100 °C.

For the identification and quantification of reaction products, the mixtures were analyzed using HPLC and ESI-MS techniques. HPLC and ESI-MS analysis confirmed that glycine oligomerized into peptides up to tetramers, while alanine primarily formed dimers. Fig. 7(a–d) and 8(a–d) represent the HPLC chromatogram showing the separation of DKP, oligomers of glycine, and alanine at optimal conditions. The reaction was conducted at temperatures ranging from 60 to 120 °C over five weeks without applying a dry/wetting cycle, and progress was monitored weekly. The formation of DKP(Gly) and DKP(Ala) on MHCCo complexes was found to be thermodynamically and kinetically favorable. DKP(Gly) and DKP(Ala) showed high yields, due to the low concentration of the aqua layer on the MHCCo surface as compared to the surrounding temperature at 120 °C, which does not favor elongation but instead supports the removal of water molecules from the dimeric glycine and alanine. Our findings indicated that higher temperatures favor DKP formation, consistent with previous studies.[34,50,81] Additionally, under hydrothermal conditions, the reaction rates for dimer and DKP formation were studied by Kawamura and coworkers.[82,83]

DKP played a crucial role in prebiotic chemistry in the formation and deformation of oligopeptides. It was also found that the formation of DKP is considered a dead end. The activation of dipeptides was studied from the perspective of the

 © 2025 The Author(s). Published by the Royal Society of Chemistry

Open Access Article. Published on 12 March 2025. Downloaded on 2/9/2026 5:05:38 PM.
This article is licensed under a Creative Commons Attribution-NonCommercial 3.0 Unported Licence.

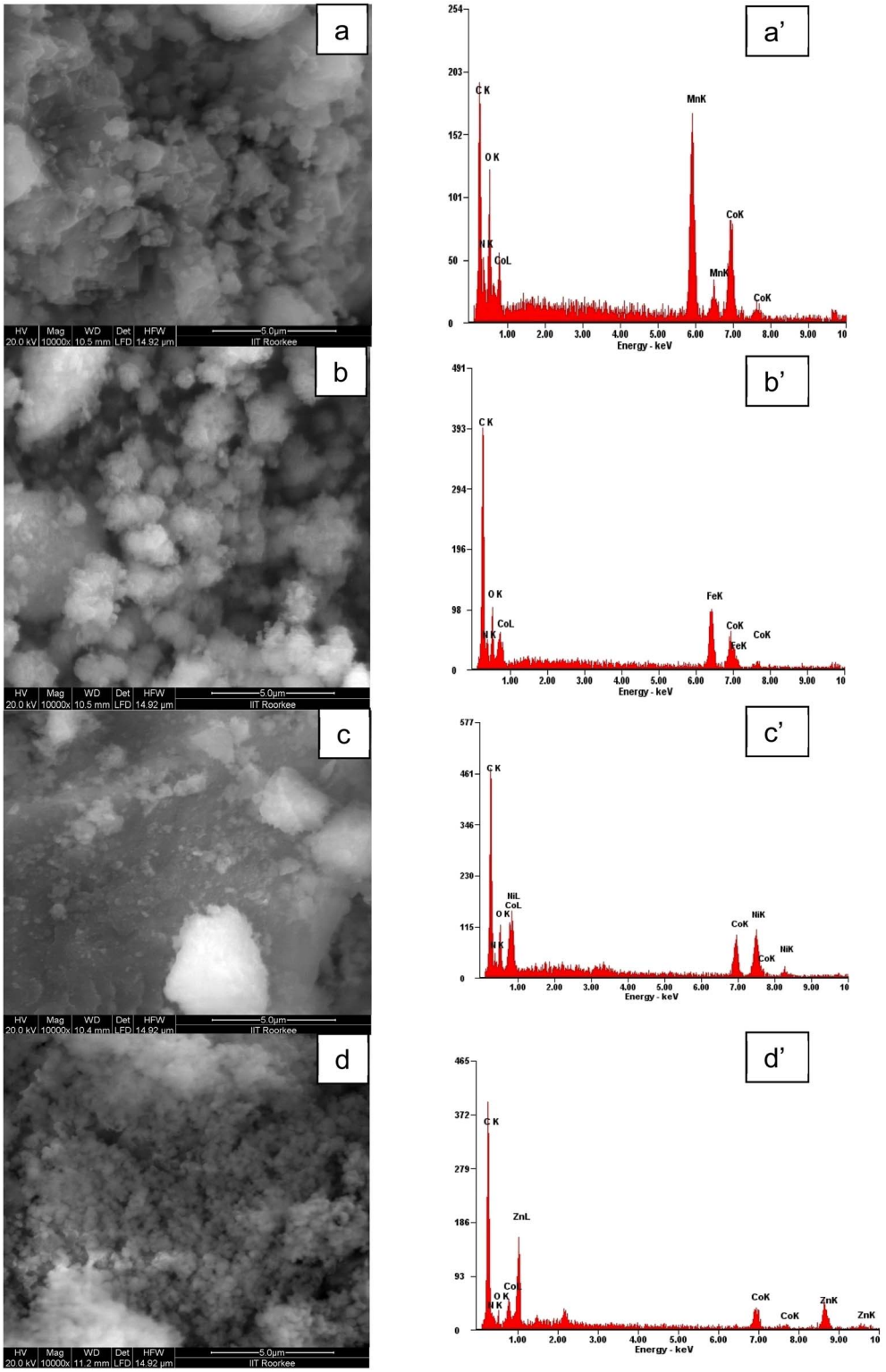

Fig. 2 FE-SEM images and EDX spectra of (a) MnHCCo; (b) FeHCCo; (c) NiHCCo; (d) ZnHCCo.

abiotic formation of oligopeptides of significant length as a requirement for secondary structure formation. When activating free dipeptides, it was shown in this work to be efficiently suppressed.[84] Thomas (2018) reported that the K^+ ion promoted the breakdown of DKP into linear dipeptides and slows down the conversion of linear dipeptide into free amino acids when compared to Na^+.[85] Sakhno *et al.* (2019) found a very interesting study showing that the formation of linear oligopeptides occurs at a high yield in the presence of a mixture of amino acid (Glu + Leu/SiO_2) rather than single AA systems, (Glu/SiO_2, Leu/SiO_2,

Open Access Article. Published on 12 March 2025. Downloaded on 2/9/2026 5:05:38 PM.
This article is licensed under a Creative Commons Attribution-NonCommercial 3.0 Unported Licence.

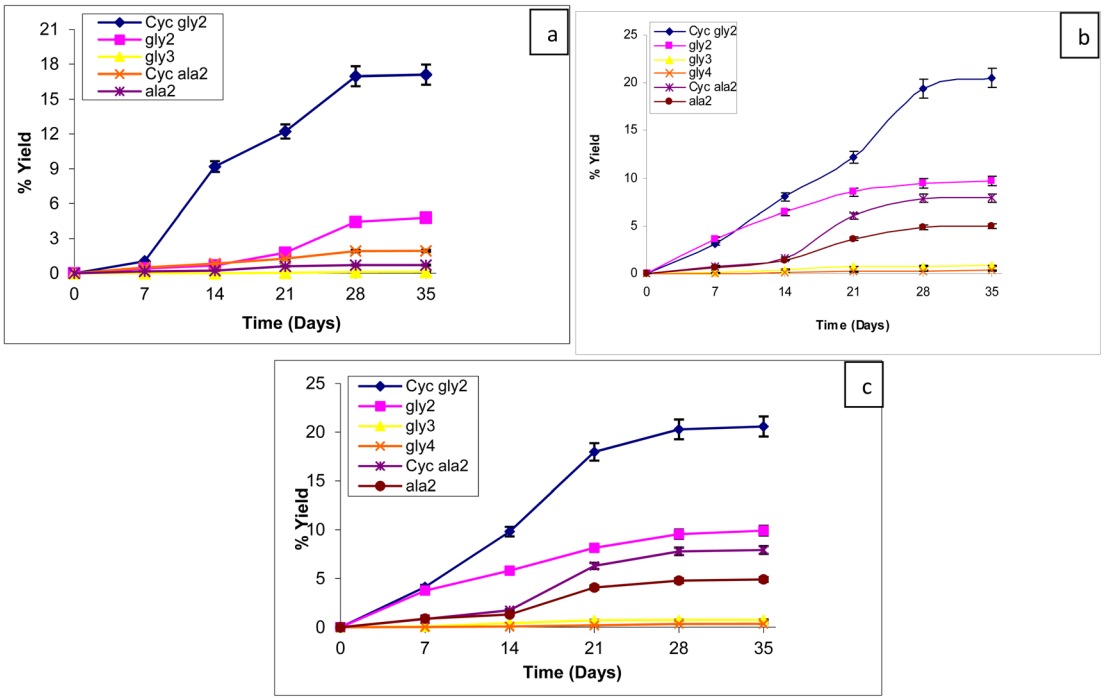

Fig. 3 Oligomerization of amino acid on MnHCCo complexes at [a] 60 °C, [b] 90 °C, [c] 120 °C.

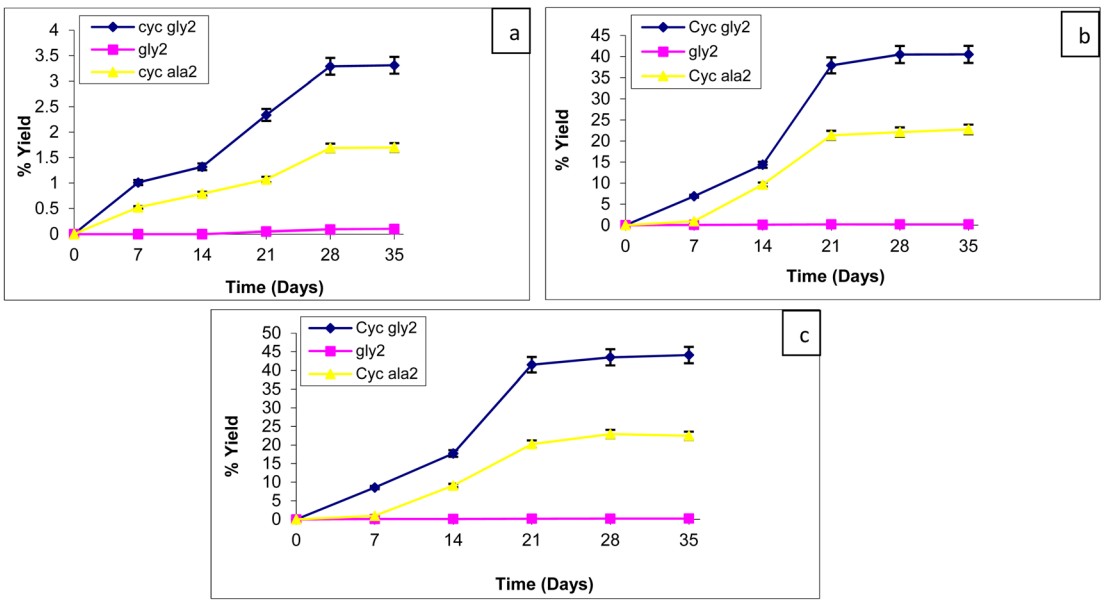

Fig. 4 Oligomerization of amino acid on FeHCCo complexes at [a] 60 °C, [b] 90 °C, [c] 120 °C.

and Val/SiO_2). While the formation of peptide bonds in these conditions has already been demonstrated many times, the main product is generally the rather uninteresting cyclic dimer DKP[86] while Bedoin *et al.* (2020) reported that at moderate temperatures, activation of leucine + glutamic acid mixtures occurs.[87]

Double metal cyanide (DMC), with general formula $M_a^I[M^{II}(CN)_n]_b \cdot xH_2O$, is an inorganic coordinated complex featuring a three dimensional network. In DMC, the inner metal M^{II} is connected to the external metal M^I through cyano-bridges (M^{II}–C≡N–M^I) where M^I = divalent metal ions such as Zn^{2+}, Fe^{2+}, Cd^{2+}, Co^{2+}, Cu^{2+}, Ni^{2+}, Mn^{2+}, *etc.* while M^{II} includes transition metal like Fe^{2+}, Fe^{3+}, Co^{2+}, Ni^{2+}, Cr^{3+}, Mo^{4+}, *etc.* The catalytic activity of DMC primarily depends on the external metal M^I, which serves as the active site. It was examined that DMC having various inner and outer sphere metals exhibited different catalytic properties. When zinc is the external metal in octacyanomolybdate(IV), the complex exhibited enhanced

© 2025 The Author(s). Published by the Royal Society of Chemistry

Open Access Article. Published on 12 March 2025. Downloaded on 2/9/2026 5:05:38 PM.
This article is licensed under a Creative Commons Attribution-NonCommercial 3.0 Unported Licence.

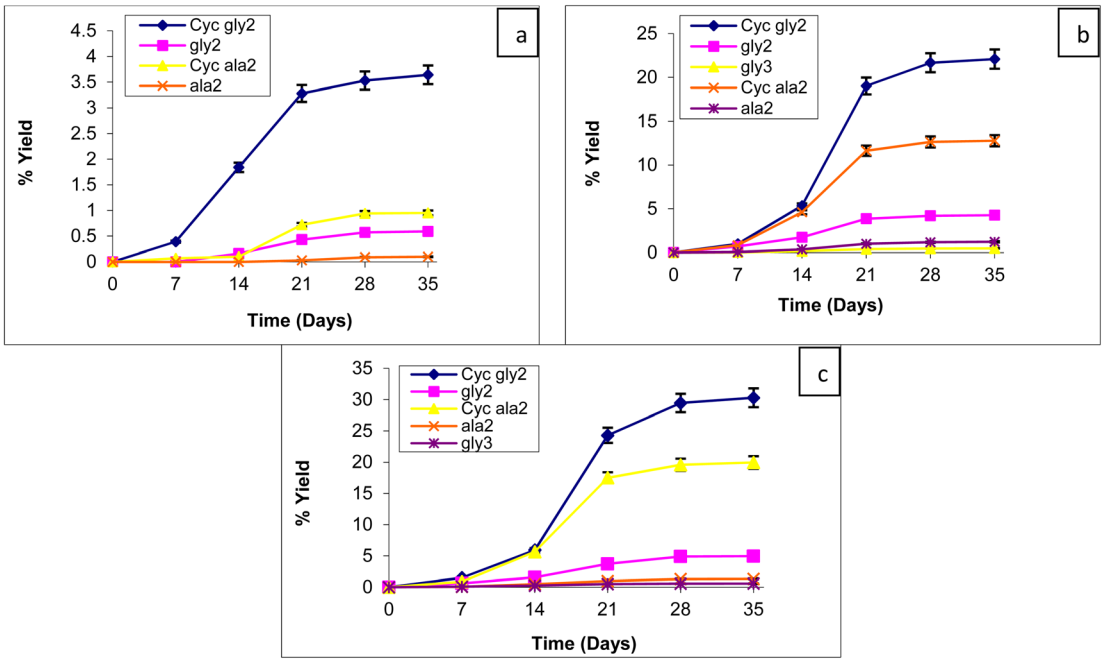

Fig. 5 Oligomerization of amino acid on NiHCCo complexes at [a] 60 °C, [b] 90 °C, [c] 120 °C.

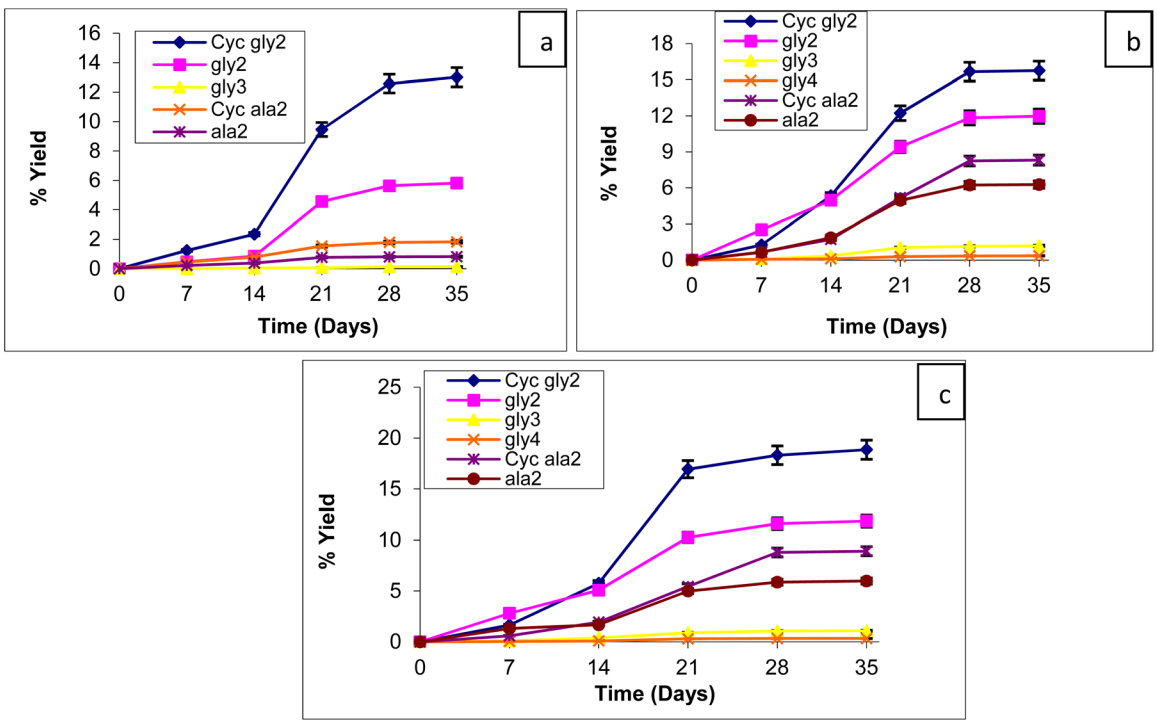

Fig. 6 Oligomerization of amino acid on ZnHCCo complexes at [a] 60 °C, [b] 90 °C, [c] 120 °C.

catalytic activity for the oligomerization of glycine and alanine compared to other metals such as Mn^{2+}, Fe^{2+}, Co^{2+}, Ni^{2+}, Cu^{2+}, and Cd^{2+}.[34] Similarly, hexacyanocobaltate complexes with zinc as the external metal also demonstrate superior catalytic efficiency in forming glycine and alanine oligomers compared to those containing Mn^{2+}, Fe^{2+}, or Ni^{2+} in the outer sphere.

Tables 2 and 3 present the percentage yield of Cyclic $(Gly)_2$, di-, tri-, a tetramer forms of glycine, and Cyclic $(Ala)_2$, a dimer of alanine on the surface of MHCCo complexes. It was observed that ZnHCCo and MnHCCo facilitate glycine oligomerization up to tetramer stage, whereas NiHCCo supports oligomerization up to the trimer, and FeHCCo only up to the dimer.

© 2025 The Author(s). Published by the Royal Society of Chemistry

Open Access Article. Published on 12 March 2025. Downloaded on 2/9/2026 5:05:38 PM. This article is licensed under a Creative Commons Attribution-NonCommercial 3.0 Unported Licence.

Table 2 Percent yield (%) of obtained products from glycine

Percent yield of obtained products from glycine at different temperatures after five weeks												
	$Cyc(Gly)_2$			$(Gly)_2$			$(Gly)_3$			$(Gly)_4$		
Catalyst	60°	90°	120°	60°	90°	120°	60°	90°	120°	60°	90°	120°
No catalyst	0.04	0.06	0.10	Trace	0.02	0.03	—	—	—	—	—	—
MnHCCo	17.11	20.55	20.58	4.79	9.73	9.92	0.12	0.81	0.76	—	0.32	0.35
FeHCCo	3.31	40.50	44.11	0.10	0.20	0.22	—	—	—	—	—	—
NiHCCo	3.64	22.08	30.29	0.59	4.26	4.94	—	0.47	0.58	—	—	—
ZnHCCo	13.01	15.73	18.85	5.81	11.97	11.87	0.14	1.19	1.09	—	0.36	0.34

Table 3 Percent yield (%) of obtained products from alanine

Percent yield of obtained products from alanine at different temperatures after five weeks						
	$Cyc(Ala)_2$			$(Ala)_2$		
Catalyst	60°	90°	120°	60°	90°	120°
No catalyst	0.02	0.04	0.06	—	—	—
MnHCCo	1.94	7.90	7.93	0.71	4.96	4.91
FeHCCo	1.70	22.76	22.47	—	—	—
NiHCCo	0.95	12.78	19.96	0.10	1.22	1.32
ZnHCCo	1.83	8.31	8.91	0.82	6.27	5.98

ZnHCCo complex formed $(Gly)_4$ (0.36%), $(Gly)_3$(1.19%), $(Gly)_2$(11.97%), DKP(Gly)(15.73%) from glycine while alanine oligomerization resulted in $(Ala)_2$ (6.27%), and $Cyclic(Ala)_2$(8.31%) after 35 days at 90 °C. Kitadai *et al.* (2016) observed the oligomerization of glycine on nine oxide minerals, out of which rutile showed the maximum catalytic activity for the formation of $(Gly)_5$ form glycine at 80 °C within 10 days.[88] Similarly, McKee evaluated the production of amide/ester-linked oligomers under simple low temperature (85 °C) evaporative conditions in silica using the α-hydroxy acids L-lactic acid and either L-alanine or glycine. AA-enriched oligomers exceeding 10 glycine residues and up to 7 alanine residues were

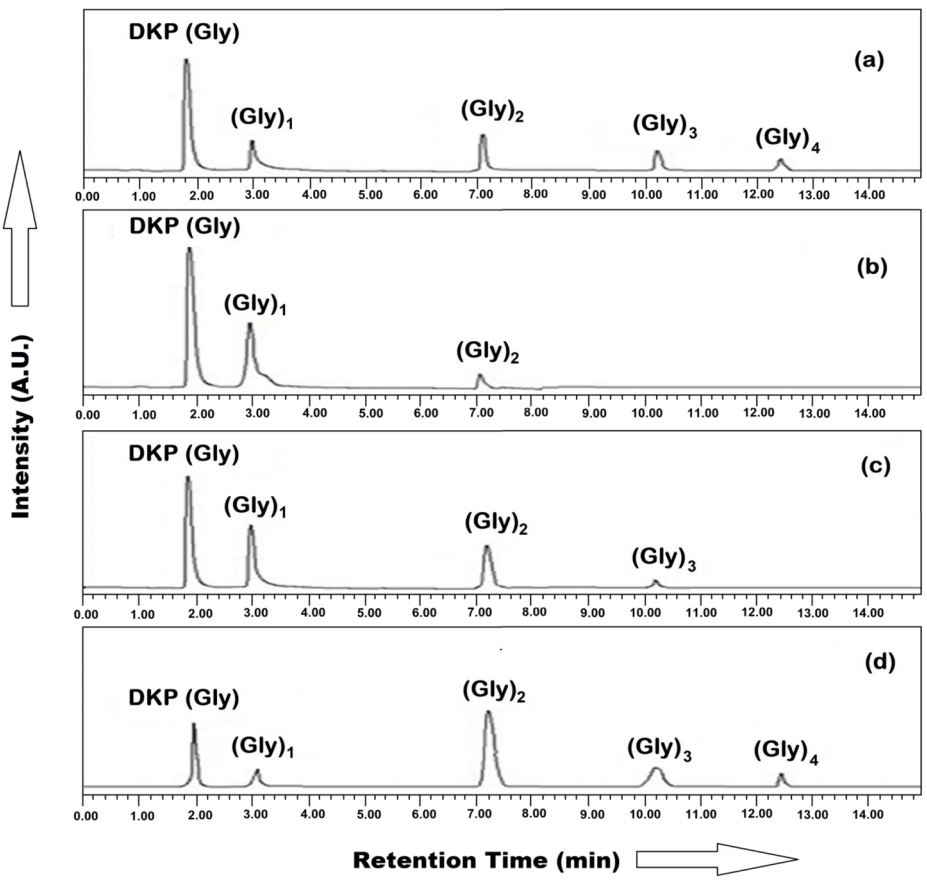

Fig. 7 HPLC chromatogram showing the products formed on the surface of (a) MnHCCo, (b) FeHCCo, (c) NiHCCo, (d) ZnHCCo when glycine was heated at 90 °C after four weeks. Retention times of analyzed products (min): Cyc $(Gly)_2$ (1.94), Gly (3.04), $(Gly)_2$ (7.12), $(Gly)_3$ (10.17), $(Gly)_4$ (12.35).

 © 2025 The Author(s). Published by the Royal Society of Chemistry

Open Access Article. Published on 12 March 2025. Downloaded on 2/9/2026 5:05:38 PM.
This article is licensed under a Creative Commons Attribution-NonCommercial 3.0 Unported Licence.

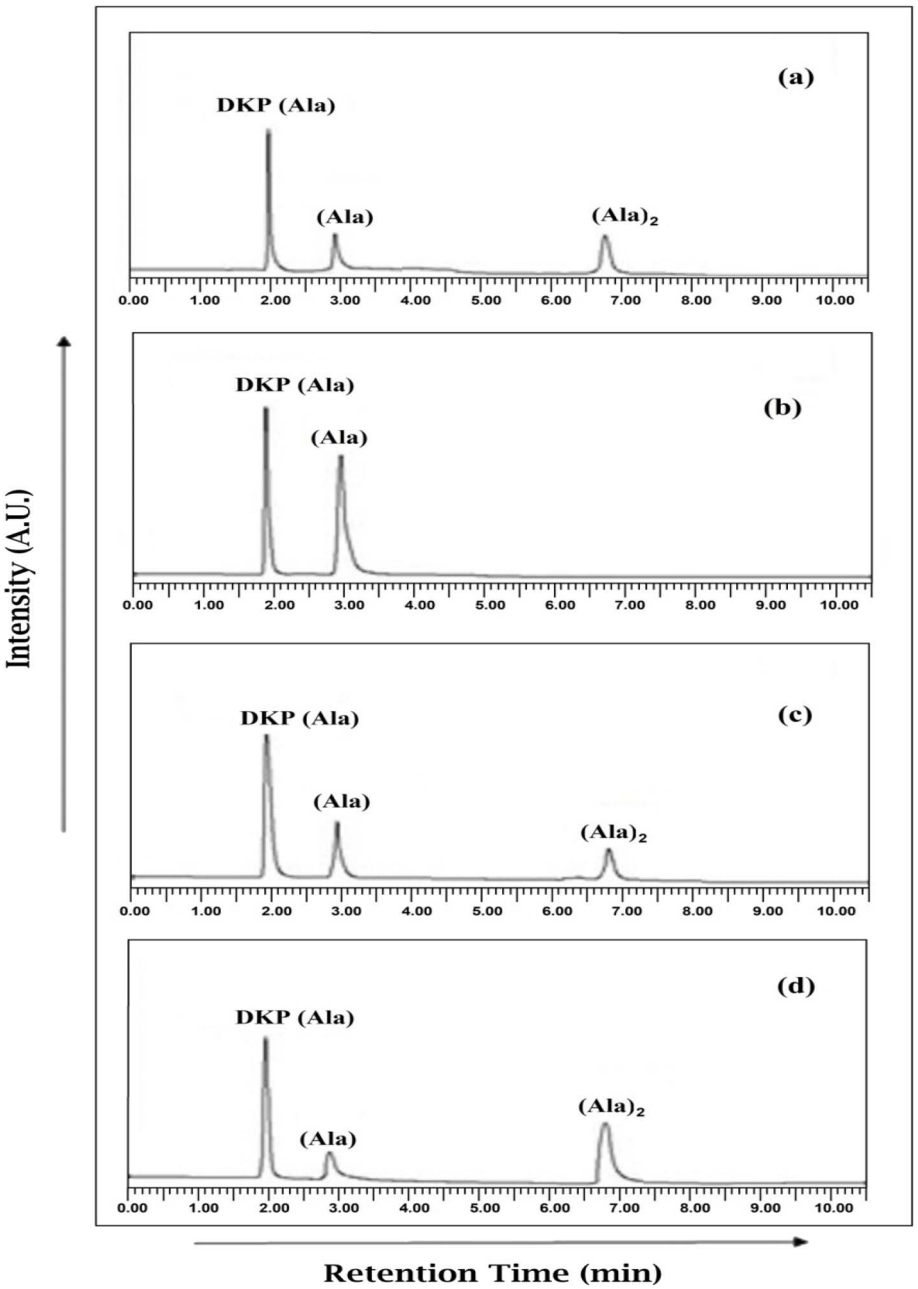

Fig. 8 HPLC chromatogram showing the products formed on the surface of (a) MnHCCo, (b) FeHCCo, (c) NiHCCo, (d) ZnHCCo when alanine was heated at 90 °C after four weeks. Retention times of analyzed products (min): Cyc $(ala)_2$ (1.95), ala (2.91), $(ala)_2$ (6.74).

produced.[89] In the present study, we also revealed that the yield of the glycine oligomer in the presence of MHCCo complexes is much higher than that of the oligomer of alanine, due to the high activation energy required for alanine oligomerization.[90] The lower amount and efficiency of catalytic sites is the another factor that can be responsible for the lower oligomerization of alanine on MHCCo complexes.[91] Greenstein reported that the stability constants of coordination complexes with amino acids are higher than the peptides that support the formation of an oligomer of glycine and alanine.[92] This mechanism revealed that as the chain length of amino acids elongates, oligomer concentration decreases (Tables 2 and 3).

Sakhno *et al.* (2019) showed the three mechanisms involved in adsorption and oligomerization processes: (i) competitive adsorption; (ii) independent adsorption; (iii) cooperative adsorption. They found that in a single amino acid (AA) system, competitive and independent adsorption mechanisms dominate, resulting in a lower yield of linear oligopeptides and a higher yield of DKP. The cooperative adsorption mechanism is likely more effective in the Glu + Leu/SiO_2 and Asp + Val/SiO_2 *i.e.* in different AA systems. MHCCo complexes follow the competitive adsorption and independent adsorption mechanisms as they involved a single AA system and give oligomers up to tetramers only and a high DKP yield.[86] The basis of the

Open Access Article. Published on 12 March 2025. Downloaded on 2/9/2026 5:05:38 PM. This article is licensed under a Creative Commons Attribution-NonCommercial 3.0 Unported Licence.

Table 4 Surface area of MHCCo complexes

MHCCo complexes	Surface area ($m^2\ g^{-1}$)
$Mn_3[Co(CN)_6]_2 \cdot 2H_2O$	615.26
$Fe_3[Co(CN)_6]_2 \cdot 3H_2O$	167.91
$Ni_3[Co(CN)_6]_2 \cdot 3H_2O$	572.39
$Zn_3[Co(CN)_6]_2 \cdot 4H_2O$	683.17

% yield of glycine and alanine oligomers in the presence of MHCCo complexes shows the following catalytic activity trend:

ZnHCCo > MnHCCo > NiHCCo > FeHCCo.

The surface area of MHCCo complexes (Table 4) and the yield of peptide bond formation (Tables 2 and 3), suggested that the surface area of MHCCo complexes plays an important parameter for the polymerization of amino acids. Among MHCCo, ZnHCCo has the highest surface area (683 $m^2\ g^{-1}$) and showed high catalytic activity for peptide bond formation, while FeHCCo has a lower surface area (S. A = 167 $m^2\ g^{-1}$) and exhibited minimum catalytic activity for the formation of linear oligopeptides.

The ESI-MS technique provides an additional analytical technique for the detection of oligomers of glycine and alanine in terms of mass, $m/z = (M + H)^+$ ions, where M indicates the amino acid or oligomers to be analyzed. Fig. 9(a) and (b) represent the ESI-MS spectrum of the formation of oligomers of glycine and alanine, respectively, on the surface of ZnHCCo at the optimal temperature after four weeks. The ESI-MS (Fig. 9(a)) confirmed the formation of DKP (glycine), dimer, trimer, and tetramer of glycine. The mass peaks observed include 76.1 of $[Gly + H]^+$, 115 for $[CycGly_2 + H]^+$, 132.9 for $[Gly_2 + H]^+$, 189.9 for $[Gly_3 + H]^+$, and 246.6 for $[Gly_4 + H]^+$. Similarly, Fig. 9(b) presents the ESI-MS spectrum for alanine oligomerization on ZnHCCo, confirming the formation of DKP (alanine), a dimer of alanine at the optimum temperature after four weeks. The observed mass includes 90.1 for $[Ala + H]^+$, 143 for $[CycAla_2 + H]^+$ and 160.9 for $[ala_2 + H]^+$. Both ESI-MS and HPLC data matched the results obtained throughout the experiments.

Divalent transition metal hexacyanocobaltates(III), in which the central metal atom and carbon of the cyanide group are bonded through the coordinate bond. It is found that these porous, water-insoluble, mixed valency octahedral coordinated complexes are a part of the *Fm*3*m* and *Pm*3*m* space groups.[72,93] The mixed metal hexacyanides usually have *Fm*3*m* and *Pm*3*m* space groups. Mixed (Fe^{2+} and Cu^{2+}) double metal hexacyanocobaltates as solid catalysts for the aerobic oxidation of oximes to carbonyl compounds.[94] It has also been observed that generally mixed metal hexacyanides show high catalytic activity, which promoted by reduced size.[72,95–97]

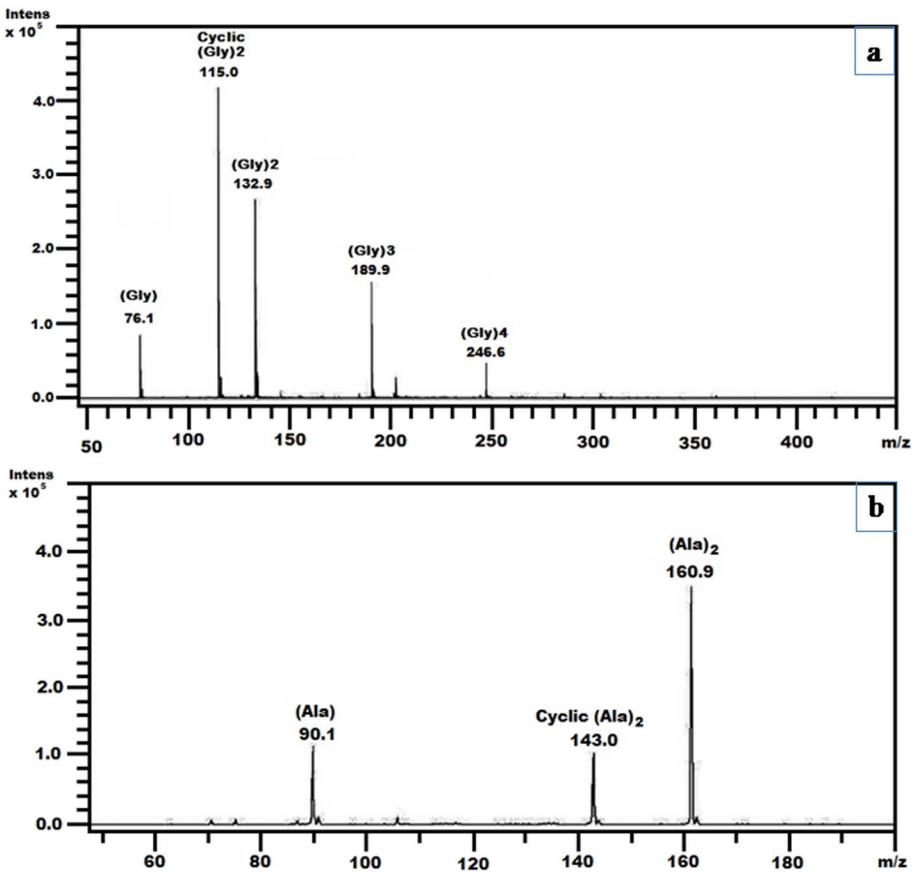

Fig. 9 ESI MS spectra of obtained products on surface of ZnHCCo complexes when (a) glycine and (b) alanine were heated at 90 °C after four weeks.

© 2025 The Author(s). Published by the Royal Society of Chemistry

Open Access Article. Published on 12 March 2025. Downloaded on 2/9/2026 5:05:38 PM.
This article is licensed under a Creative Commons Attribution-NonCommercial 3.0 Unported Licence.

MHCCo complexes provide active sites for the adsorption of amino acids due to the presence of divalent metal ions (M^{2+}), which act as Lewis acids. The adsorption process primarily involves the formation of coordination bonds between these M^{2+} ions and the functional groups of amino acids, particularly the carboxylate ($-COO^-$) group. This interaction stabilizes the amino acid on the catalyst surface, orienting it in a way that facilitates subsequent chemical reactions.

Upon coordination, the electronic environment of the amino acid is significantly altered. The metal ion polarizes the carboxylate group, increasing the electrophilicity of the carbonyl carbon. Simultaneously, the electron-withdrawing

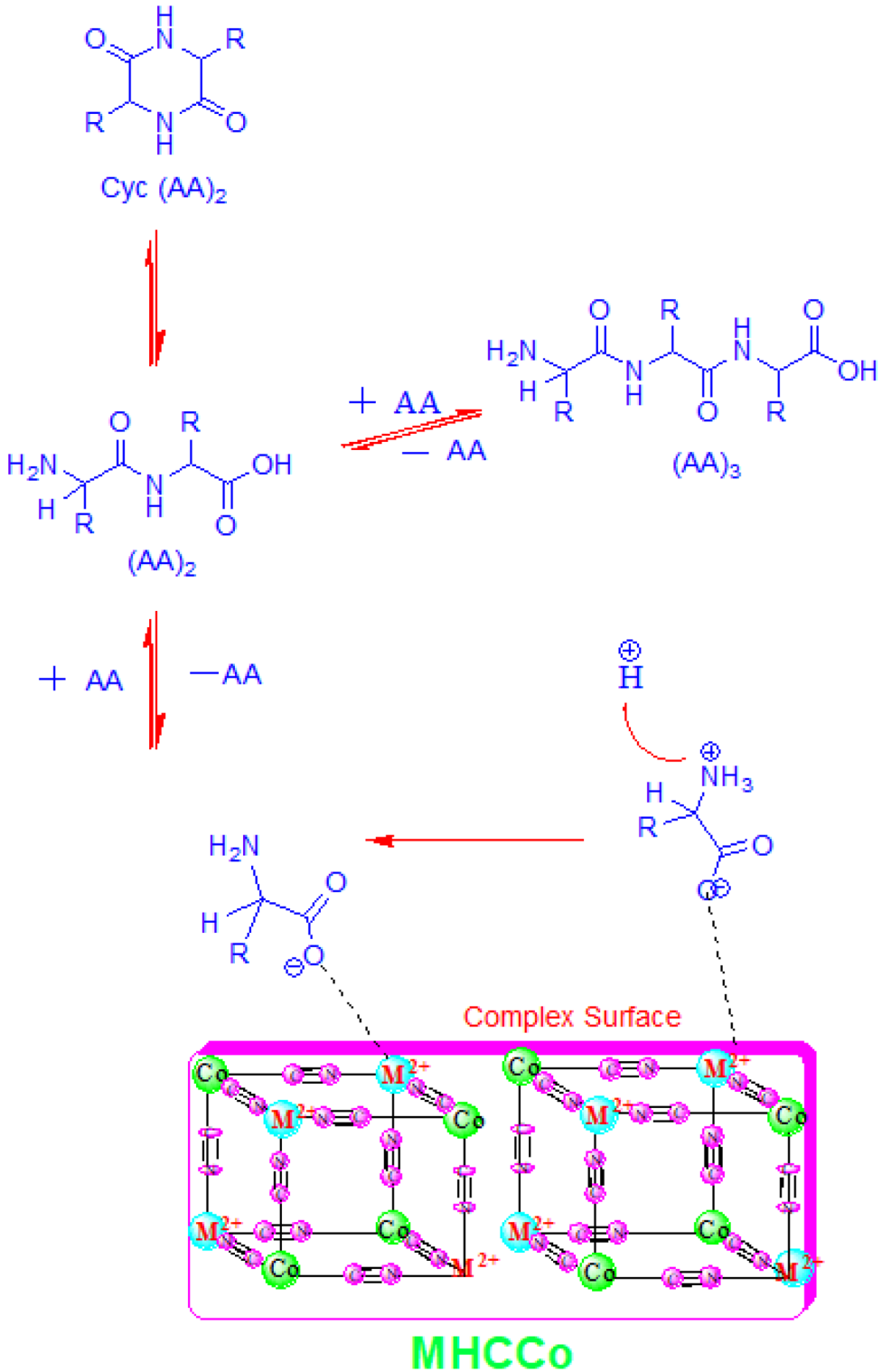

Fig. 10 Proposed pathway for the oligomerization of glycine and alanine in the presence of MHCCo complexes.

Open Access Article. Published on 12 March 2025. Downloaded on 2/9/2026 5:05:38 PM. This article is licensed under a Creative Commons Attribution-NonCommercial 3.0 Unported Licence.

effect of the metal ion coordination enhances the nucleophilicity of the amino group (–NH_2) by reducing electron density around the carboxyl group, thereby making the lone pair of electrons on the nitrogen more available for nucleophilic attack. This activation leads to a key step in the oligomerization mechanism: the nucleophilic attack of the amino group from one amino acid molecule on the carbonyl carbon of another amino acid molecule's carboxyl group. The reaction proceeds through the formation of a intermediate complex, where the metal ion continues to stabilize the developing negative charge on the oxygen atom of the carbonyl group.

Following the formation of this intermediate, a condensation reaction occurs, resulting in the formation of a peptide bond (–CO–NH–) and the release of a water molecule. The metal ion not only facilitates the nucleophilic attack but also stabilizes transition states and intermediates, lowering the activation energy required for peptide bond formation. This mechanism enables the stepwise formation of oligopeptides, with the MHCCo complexes acting as heterogeneous catalysts. The ability of these complexes to repeatedly adsorb, activate, and facilitate reactions between amino acid molecules underpins their efficiency in promoting oligomerization reactions.

The proposed mechanism for the oligomerization of amino acids catalyzed by MHCCo complexes is depicted in Fig. 10, illustrating the adsorption, activation, nucleophilic attack, intermediate formation, and eventual peptide bond creation.

In the present study, MHCCo complexes also showed catalytic activity for the production of peptide bond formations because of their mixed valency and high surface area. The evidence summarized above suggested the catalytic activity of MHCCo complexes for the condensation of amino acids and thus supports the chemical evolution of life.

4. Conclusion

The present results support the catalytic behavior of MHCCo for amino acid oligomerization. This is the first time that MHCCo has been investigated for the oligomerization of glycine and alanine along with parameters such as time duration and temperature. It is found that hexacyanocobalte having zinc as an outer sphere metal *i.e.* ZnHCCo acts as the most effective for adsorption and forms considerable amount of up to (0.36%) $(Gly)_4$ along with (1.19%) $(Gly)_3$, (11.97%) $(Gly)_2$ and (15.75%) Cyclic $(Gly)_2$ while in case of alanine (6.27%) $(Ala)_2$ and (8.31%) Cyclic$(Ala)_2$ while the hexacyanocobalte having iron as an outer sphere metal *i.e.* FeHCCo exhibited the least catalytic activity for the oligomerization process, only form (Gly) with the yield of 0.20% at moderate temperature *i.e.* at 90 °C after four weeks. High surface area is the main parameter, which provides more area for chain elongation of glycine and alanine thus a high yield of oligomers of amino acids on the surface of ZnHCCo compared to other MHCCo complexes. All MHCCo complexes give a high yield of DKP because of competitive and independent adsorption mechanisms, as it contains a single AA system. The findings showed that MHCCo in the early oceans created a surface that helped protect and stabilize amino acids. This made it easier for these amino acids to link together and form prebiotic peptide bond, which is one of the important steps in the development of life.

Data availability

All the data of this study are provided in the manuscript as well as ESI.†

Conflicts of interest

None to declare.

Acknowledgements

The author (Dr Anand Kumar) is thankful to the Ministry of Human Resource and Development (MHRD), New Delhi for providing financial assistance. The authors are also thankful to Prof. Tokeer Ahmad, Department of Chemistry, Jamia Millia Islamia, New Delhi, for the surface area analysis of the samples. The KSU author acknowledges the funding from Researchers Supporting Project number (RSP2025R355), King Saud University, Riyadh, Saudi Arabia.

References

1 A. I. Oparin, *The Origin of Life*, Moscow, p. 1936.
2 A. Utiérrez-Preciado, H. Romero and M. Peimbert, *Nat. Educ.*, 2010, **3**(9), 29.
3 K. Norio and M. Shigenori, *Geosci. Front.*, 2018, **9**(4), 1117–1153.
4 S. Jheeta, C. Elias, D. Kevin and B. Janice, *Life*, 2021, **11**(9), 872.
5 J. R. Cronin and S. Pizzarello, *Adv. Space Res.*, 1983, **3**(9), 5–18.
6 N. Kitadai and S. Maruyama, *Geosci. Front.*, 2018, **9**(4), 1117–1153.
7 J. E. Elsila, J. C. Aponte, D. G. Blackmond, A. S. Burton, J. P. Dworkin and D. P. Glavin, *ACS Cent. Sci.*, 2016, **2**(6), 370–379.
8 J. L. Bada, *Philosophical Transactions: Biol. Sci.*, 1991, **333**(1268), 349–358.
9 A. S. Burton, J. C. Stern, J. E. Elsila, D. P. Glavin and J. P. Dworkin, *Chem. Soc. Rev.*, 2012, **41**(6), 5459–5472.
10 K. Ikehara, *Chem. Rec.*, 2005, **5**, 107–118.
11 C. P. J. Maury, M. Liljestrom and F. Zhao, *J. Biol. Res.*, 2012, **18**, 332–335.
12 V. P. Gulik, S. Massar, D. Gilis, H. Buhrman and M. Rooman, *J. Theor. Biol.*, 2009, **261**, 531–539.
13 K. Ikehara, Y. Omori, R. Arai and A. Hirose, *J. Mol. Evol.*, 2002, **54**, 530–538.
14 K. Ikehara, *Int. J. Mol. Sci.*, 2009, **10**(4), 1525–1537.
15 K. Ikehara, *Chemical Models and Early Biological Evolution*, ed. J. Seckbach, Springer, 2012, 107–121.
16 K. Ikehara, *Origins Life Evol. Biospheres*, 2014, **44**(4), 299–302.
17 S. L. Miller, *Science*, 1953, **117**, 528–529.
18 A. Lazcano and J. L. Bada, *Origins Life Evol. Biospheres*, 2003, **33**, 235–242.

© 2025 The Author(s). Published by the Royal Society of Chemistry

Open Access Article. Published on 12 March 2025. Downloaded on 2/9/2026 5:05:38 PM. This article is licensed under a Creative Commons Attribution-NonCommercial 3.0 Unported Licence.

19 J. L. Bada, *Nat. Commun.*, 2023, **14**, 2011.
20 J. F. Kasting, *Spec. Pap.–Geol. Soc. Am.*, 2014, **504**, 19–28.
21 J. L. Bada, *Chem. Soc. Rev.*, 2013, **42**, 2186–2196.
22 R. Stribling and S. L. Miller, *Origins Life Evol. Biospheres*, 1987, **17**, 261–273.
23 N. Lahav and S. Chang, *J. Mol. Evol.*, 1976, **8**, 357–380.
24 J. Darnell, H. Lodish and D. Baltimore, *Molecular Cell Biology. Scientific American Books*, New York, 5th edn, 2003, pp. 29–55.
25 J. Goscianska, A. Olejnik and R. Pietrzak, *Mater. Chem. Phys.*, 2013, **142**, 586–593.
26 T. D. Campbell, R. Febrian, H. E. Kleinschmidt, K. A. Smith and P. J. Bracher, *ACS Omega*, 2019, **4**(7), 12745–12752.
27 J. F. Lambert, *Origins Life Evol. Biospheres*, 2008, **38**, 211–242.
28 B. B. Tewari and N. Hamid, *Colloids Surf., A*, 2007, **296**, 264–269.
29 J. D. Bernal, *The Physical Basis of Life*, Rourledge and Kegan Paul, London 1951, 1–80.
30 H. J. Cleaves, A. M. Scott, F. C. Hill, J. Leszczynski, N. Sahai and R. Hazen, *Chem. Soc. Rev.*, 2012, **41**, 5502–5525.
31 V. Erastova, M. T. Degiacomi, D. G. Fraser and H. C. Greenwell, *Nat. Commun.*, 2017, **8**, 2033–2042.
32 J. Goscianska, A. Olejnik and R. Pietrzak, *Mater. Chem. Phys.*, 2013, **142**, 586–593.
33 Q. Gao, Y. Xu, D. Wu and Y. Sun, *Stud. Surf. Sci. Catal.*, 2007, **170**, 961–966.
34 A. Kumar and Kamaluddin, *Amino Acids*, 2012, **43**, 2417–2429.
35 B. Saroha, A. Kumar, R. R. Maurya, M. Lal, S. Kumar, H. K. Rajouri, I. Bahadur and D. S. Negi, *J. Mol. Liq.*, 2022, **349**, 118197.
36 D. A. M. Zaia, *Amino Acids*, 2004, **27**(1), 113–118.
37 A. Kasprzhitskii, G. Lazorenko, D. S. Kharytonau, M. A. Osipenko, A. A. Kasach and I. I. Kurilo, *Appl. Clay Sci.*, 2022, **226**, 106566.
38 R. M. Hazen, T. R. Filley and G. A. Goodfriend, *Proc. Natl. Acad. Sci. U.S.A.*, 2001, **98**(10), 5487–5490.
39 S. Joshi, I. Ghosh, S. Pokhrel, L. Madler and W. M. Nau, *ACS Nano*, 2012, **6**, 5668–5679.
40 D. Costa, L. Savio and C.-M. Pradier, *J. Phys. Chem. B*, 2016, **120**(29), 7039–7052.
41 P. Stefano, R. Albert and S. Mariona, *J. Phys. Chem. A*, 2017, **121**(26), 14156–14165.
42 A. Hışır, G. K. Karaoğlan and O. Avcıata, *J. Mol. Struct.*, 2022, **1266**, 133498.
43 L. Alexandra, De. A. Francisco and N. Parac-Vogt Tatjana, *Mat. Adv.*, 2022, **3**(5), 2475–2487.
44 R. Michael and J. G. Andrew, *Surf. Sci.*, 2022, **717**, 121980.
45 N. M. Vlasova and O. V. Markitan, *Theor. Exp. Chem.*, 2022, **58**(1), 1–14.
46 W. Martin, J. Baross, D. M. Kelley and C. Russell, *Nat. Rev. Microbiol.*, 2008, **6**, 805–814.
47 E. T. Degens, J. Matheja and T. A. Jackson, *Nature*, 1970, **227**, 492–493.
48 T. L. Porter, M. P. Eastman, E. Bain and S. Begay, *Biophys. Chem.*, 2001, **91**, 115–124.
49 A. Rimola, M. Sodupe and P. Ugliengo, *J. Am. Chem. Soc.*, 2007, **129**, 8333–8344.
50 J. Wu, Z. Zhang, X. Yu, H. Pan, W. Jiang, X. Xu and R. Tang, *Chin. Sci. Bull.*, 2011, **56**, 633–639.
51 C. Zuo, B. C. Zhang, B. J. Yan and J. S. Zheng, *Org. Biomol. Chem.*, 2019, **17**, 727–744.
52 C. Ponnamperuma, A. Shimoyama and E. Friebele, *Origins Life*, 1982, **12**, 9–40.
53 N. Lahav, D. White and S. Chang, *Science*, 1978, **201**, 67–69.
54 J. J. Flores and W. A. Bonner, *J. Mol. Evol.*, 1974, **3**, 49–56.
55 J. Bujdak, H. Slosiarikova, N. Texler, M. Schwendinger and B. M. Rode, *Fur. Chemie.*, 1994, **125**, 1033–1039.
56 J. Bujdak, K. Faybikova, A. Eder, Y. Yongyai and B. M. Rode, *Origins Life Evol. Biospheres*, 1995, **25**, 431–441.
57 F. Egami, *J. Biochem.*, 1975, **77**, 1165–1169.
58 R. M. Hazen and S. M. Morrison, Mineralogical Environments of the Hadean Eon: Rare Elements Were Ubiquitous in Surface Sites of Rock-Forming Minerals, in *Prebiotic Chemistry and the Origin of Life*, ed. A. Neubeck and S. McMahon, Advances in Astrobiology and Biogeophysics, Springer, Cham, 2021, pp. 43–61.
59 R. H. Holm, P. Kennepohl and E. I. Solomon, *Chem. Rev.*, 1996, **96**(7), 2239–2314.
60 (*a*) S. Thripati and R. O. Ramabhadran, *J. Phys. Chem. A*, 2017, **121**, 8659–8674; (*b*) S. Thripati and R. O. Ramabhadran, *J. Phys. Chem. A*, 2021, **125**, 3457–3472.
61 H. Paecht-Horowitz, *Biosyst.*, 1977, **9**, 93–98.
62 L. E. Orgel, *The Origin of Life and Evolutionary Biochemistry*, ed. K. Dose, S. W. Fox, Lenum PublishingCorporation, New York, 1974, 369–371.
63 A. D. Keefe and S. L. Miller, *Origins Life Evol. Biospheres*, 1996, **26**, 111–129.
64 R. Stribling and S. L. Miller, *Origins Life Evol. Biospheres*, 1987, **17**, 261–273.
65 T. Arrhenius, G. Arrhenius and W. Paplawsky, *Origins Life Evol. Biospheres*, 1994, **24**, 1–17.
66 M. T. Beck, *Pure Appl. Chem.*, 1987, **59**(12), 1703–1720.
67 S. R. Ali and Kamaluddin, *Origins Life Evol. Biospheres*, 2007, **37**, 225–234.
68 Kamaluddin, M. Nath and A. Sharma, *Origins Life Evol. Biospheres*, 1994, **24**, 469–477.
69 S. R. Ali and Kamaluddin, *Bull. Chem. Soc. Jpn.*, 2006, **79**(10), 1541–1546.
70 A. Kumar and Kamaluddin, *Origins Life Evol. Biospheres*, 2013, **43**, 1–17.
71 R. Sharma, M. A. Iqubal, S. Jheeta and Kamaluddin, *Inorganics*, 2017, **5**(2), 18.
72 S. S. Kaye and J. R. Long, *J. Am. Chem. Soc.*, 2005, **127**, 6506–6507.
73 C. P. Krap, B. Zamora, L. Reguera and E. Reguera, *Microporous Mesoporous Mater.*, 2009, **120**, 414–420.
74 D. F. Mullica, J. D. Oliver, W. O. Milligan and F. W. Hills, *Inorg. Nucl. Chem. Lett.*, 1979, **15**, 361–365.
75 D. F. Mullica, J. T. Zielke and E. L. Sappenfield, *J. Solid State Chem.*, 1994, **112**, 92–95.
76 S. Brunauer, P. H. Emmett and E. Teller, *J. Am. Chem. Soc.*, 1938, **60**, 309–319.

Open Access Article. Published on 12 March 2025. Downloaded on 2/9/2026 5:05:38 PM.
This article is licensed under a Creative Commons Attribution-NonCommercial 3.0 Unported Licence.

77 R. Sharma, A. Kumar, M. A. Iqubal and Kamaluddin, *Astrobiol. Outreach*, 2015, **3**(4), 1000138.
78 K. Zhang, T. H. Lee, J. H. Cha, R. S. Varma, J. W. Choi, H. W. Jang and M. Shokouhimehr, *ACS Omega*, 2019, **25**(4), 21410–21416.
79 J. Bujdak and B. M. Rode, *Origins Life Evol. Biospheres*, 1999, **29**, 451–461.
80 J. Bujdak and B. M. Rode, *J. Mol. Catal. A:Chem.*, 1999, **144**, 129–136.
81 J. Bujdak and B. M. Rode, *Amino Acids*, 2001, **21**, 281–291.
82 K. Kawamura, T. Nishi and T. Sakiyama, *J. Am. Chem. Soc.*, 2005, **127**, 522–523.
83 K. Kawamura and M. Yukioka, *Thermochim. Acta*, 2001, **375**, 9–16.
84 D. Beaufils, S. Jepaul, Z. Liu, L. Boiteau and R. Pascal, *Origins Life Evol. Biospheres*, 2016, **46**, 19–30.
85 T. D. Campbell, C. A. Hart, R. Febrian, M. L. Cheneler and P. J. Bracher, *Tetrahedron Lett.*, 2018, **59**, 2264–2267.
86 Y. Sakhno, A. Battistella, A. Mezzetti, M. Jaber, T. Georgelin, L. Michot and J. F. Lambert, *Chem.–Eur. J.*, 2019, **25**, 1275–1285.
87 L. Bedoin, S. Alves and J. F. Lambert, *ACS Earth Space Chem.*, 2020, **4**(10), 1802–1812.
88 N. Kitadai, H. Oonishi, K. Umemoto, T. Usui, K. Fukushi and S. Nakashima, *Origins Life Evol. Biospheres*, 2016, **47**(2), 123–143.
89 A. D. McKee, M. Solano, A. Saydjari, C. J. Bennett, N. V. Hud and T. M. Orlando, *Chem. Bio. Chem.*, 2018, **19**(18), 1913–1917.
90 J. G. Lawless and N. Levi, *J. Mol. Evol.*, 1979, **13**, 281–286.
91 M. G. Schwendinger and B. M. Rode, *Inorg. Chim. Acta*, 1991, **186**, 247–251.
92 J. P. Greenstein and M. Winitz, *Chemistry of Amino Acids*, John Wiley & Sons, New York, 1961.
93 M. R. Hartman, V. K. Peterson, Y. Liu, S. S. Kaye and J. R. Long, *Chem. Mater.*, 2006, **18**, 3221–3224.
94 A. García-Ortiz, A. Grirrane, E. Reguera and H. García, *J. Catal.*, 2014, **311**, 386–392.
95 L. Guadagnini, D. Tonelli and M. Giorgetti, *Electrochim. Acta*, 2010, **55**, 5036–5039.
96 O. N. Risset, E. S. Knowles, S. Q. Ma, M. W. Meisel and D. R. Talham, *Chem. Mater.*, 2013, **25**, 42–47.
97 K. Zhang, R. S. Varma, H. W. Jang, J. W. Choi and M. Shokouhimehr, *J. Alloys Compd.*, 2019, **791**, 911–917.

© 2025 The Author(s). Published by the Royal Society of Chemistry